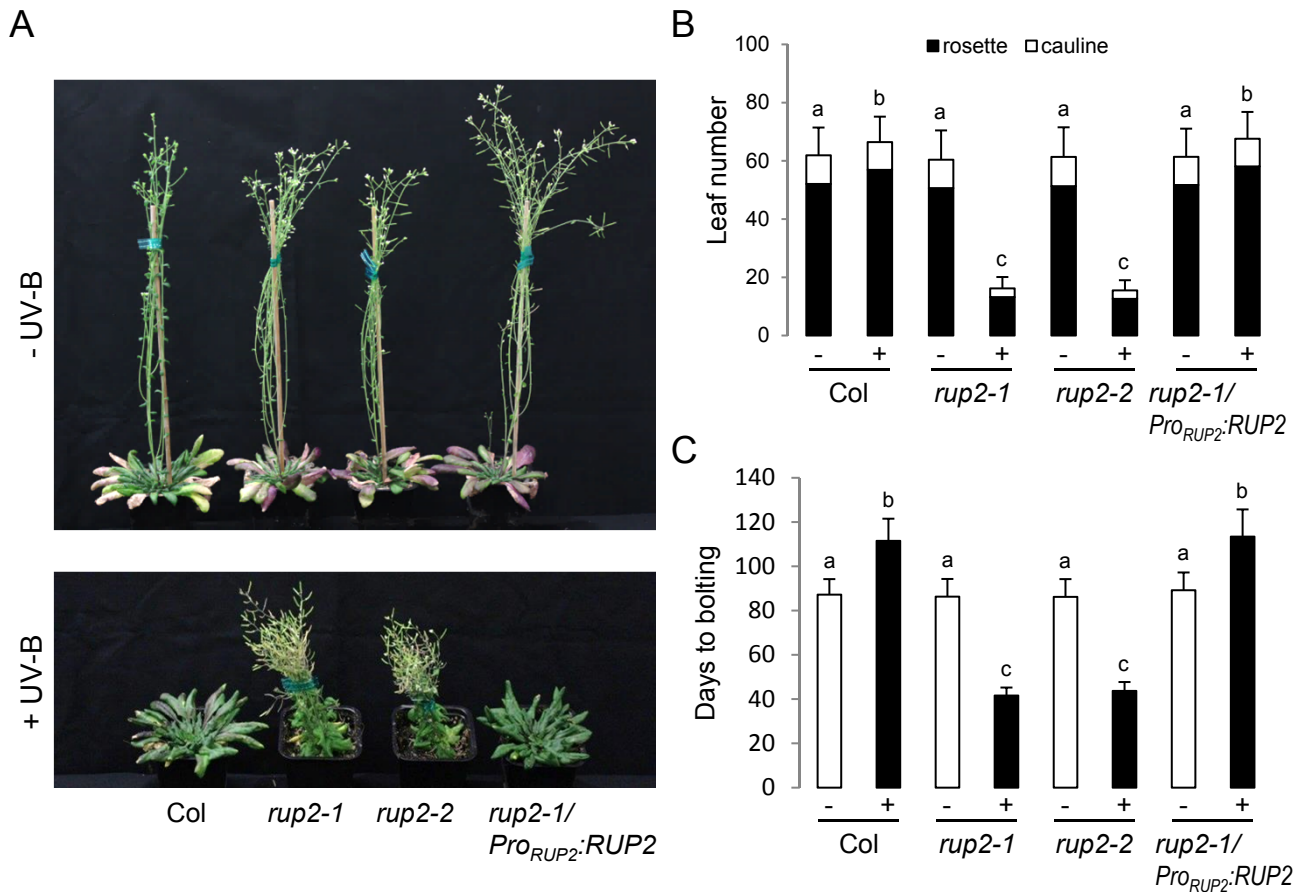
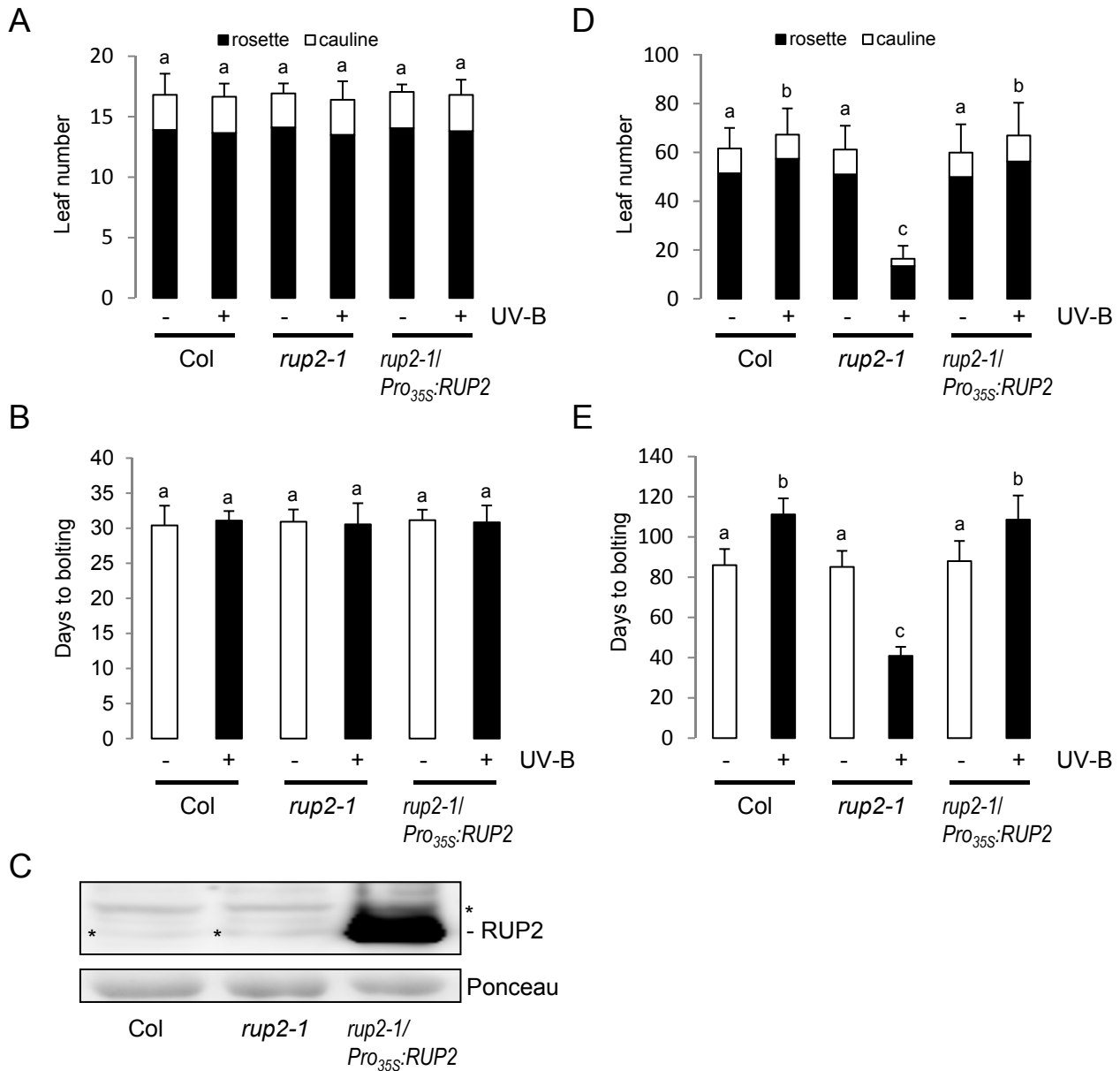


**Figure S1.** Early flowering of *rup1 rup2* double mutants in SD with UV-B is suppressed by UVR8 mutation. (A,B) Quantification of flowering time of wild-type (Col), *uvr8-6*, *rup1-1 rup2-1*, and *rup1-1 rup2-1 uvr8-6* plants grown in SD with (+) or without (-) UV-B. The flowering time is represented by total leaf number (rosette and cauline leaves; A) and days to bolting (B). Error bars represent SD ( $n = 30$ ); shared letters indicate no statistically significant difference in the means ( $P > 0.05$ ).



**Figure S2.** The novel *rup2-2* mutant allele flowers early in SD with UV-B and transgenic expression of *RUP2* complements the *rup2-1* early flowering phenotype. (A) Representative images of 100-d-old wild-type (Col), *rup2-1*, *rup2-2*, and *rup2-1/Pro<sub>RUP2</sub>:RUP2* *Arabidopsis* plants grown with (+UV-B) or without (-UV-B) UV-B (note that the *rup2-1* +UV-B plant is identical to the one shown in Fig. 1A, as from the same experiment). (B,C) Quantification of flowering time of wild-type (Col), *rup2-1*, *rup2-2*, and *rup2-1/Pro<sub>RUP2</sub>:RUP2* plants grown in SD with (+) or without (-) UV-B. The flowering time is represented by total leaf number (rosette and cauline leaves; B) and days to bolting (C). Error bars represent SD ( $n = 30$ ); shared letters indicate no statistically significant difference in the means ( $P > 0.05$ ).



**Figure S3.** *RUP2* overexpression does not affect the flowering time in LD, independent of the absence or presence of UV-B. (A,B) Quantification of flowering time of WT (Col), *rup2-1*, and *rup2-1/Pro<sub>35S</sub>:RUP2* plants grown in LD with (+) or without (-) UV-B. The flowering time is represented by total leaf number (rosette and cauline leaves; A) and days to bolting. Error bars represent SD ( $n = 30$ ). (C) Immunoblot analysis of RUP2 levels in the *rup2-1/Pro<sub>35S</sub>:RUP2* overexpression line compared to that in WT (Col) and *rup2-1*. Asterisks indicate nonspecific cross-reacting bands. The membrane was stained with Ponceau S as a loading control. (D,E) Quantification of flowering time of WT (Col), *rup2-1*, and *rup2-1/Pro<sub>35S</sub>:RUP2* plants grown in SD with (+) or without (-) UV-B. The flowering time is represented by total leaf number (rosette and cauline leaves; D) and days to bolting (E). Error bars represent SD ( $n = 24$ ).

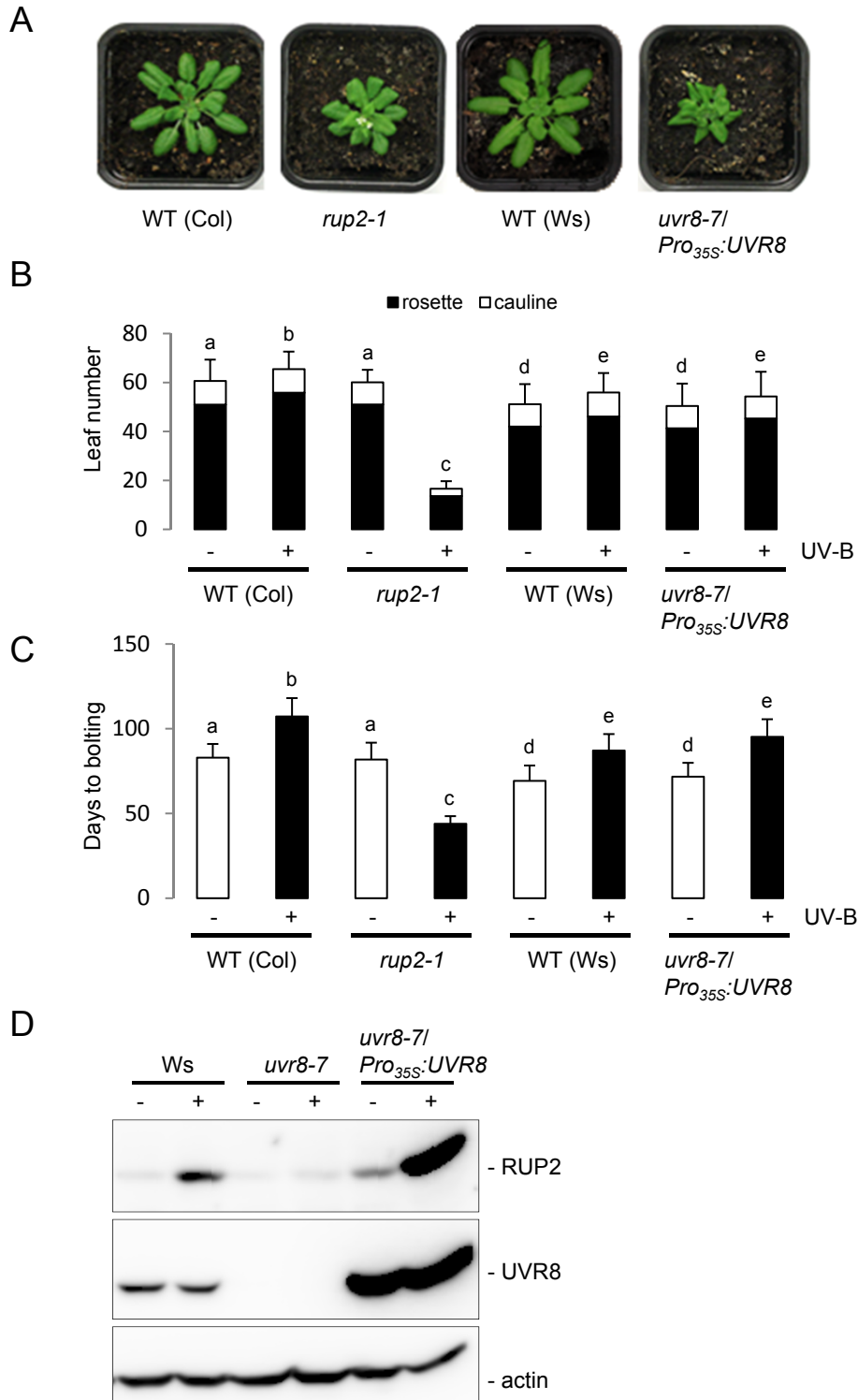


**Figure S4.** Overexpression of UVR8 results in UV-B hypersensitivity but not in an early flowering phenotype under SD+UV. (A) Representative images of 45-d-old WT (Col and Ws), *rup2-1*, and *uvr8-7/Pro<sub>35S</sub>:UVR8* plants grown under SD+UV. (B,C) Quantification of flowering time of WT (Col and Ws), *rup2-1*, and *uvr8-7/Pro<sub>35S</sub>:UVR8* plants grown in SD with (+) or without (-) UV-B. The flowering time is represented by total leaf number (rosette and cauline leaves; B) and days to bolting (C). Error bars represent SD ( $n = 30$ ); shared letters indicate no statistically significant difference in the means ( $P > 0.05$ ). (D) Immunoblot analysis of RUP2 and UVR8 protein levels in 4-d-old wild-type (Ws), *uvr8-7*, and *uvr8-7/Pro<sub>35S</sub>:UVR8* seedlings grown in the absence (-) or presence (+) of UV-B. Actin levels are shown as a loading control.

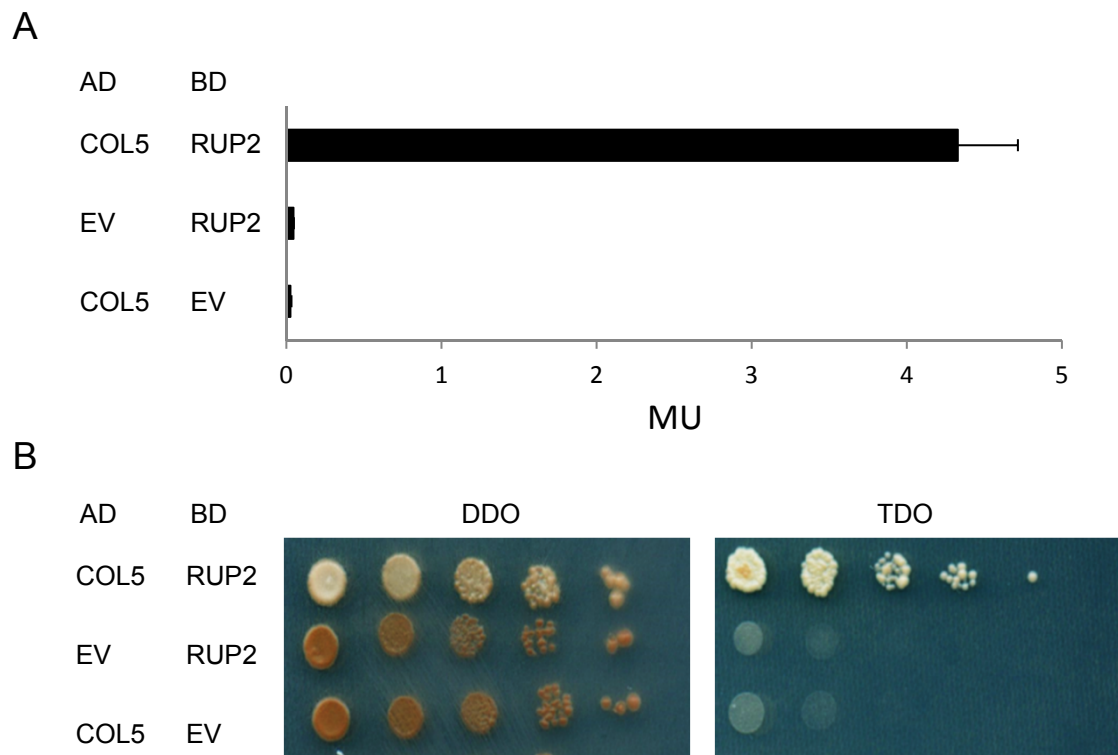


**Figure S5.** RUP2 interacts with COL5/BBX6 in yeast. (A,B) Quantitative  $\beta$ -galactosidase yeast two-hybrid activity assay (A) and growth assay of 10-fold serial dilutions on DDO (nonselective for interaction) and TDO (selective) plates (B). AD: activation domain; BD: binding domain; EV: empty vector; MU, Miller units; DDO, SD/-Trp/-Leu; TDO, SD/-Trp/-Leu/-His. Means and SEM from three biological replicates are shown.

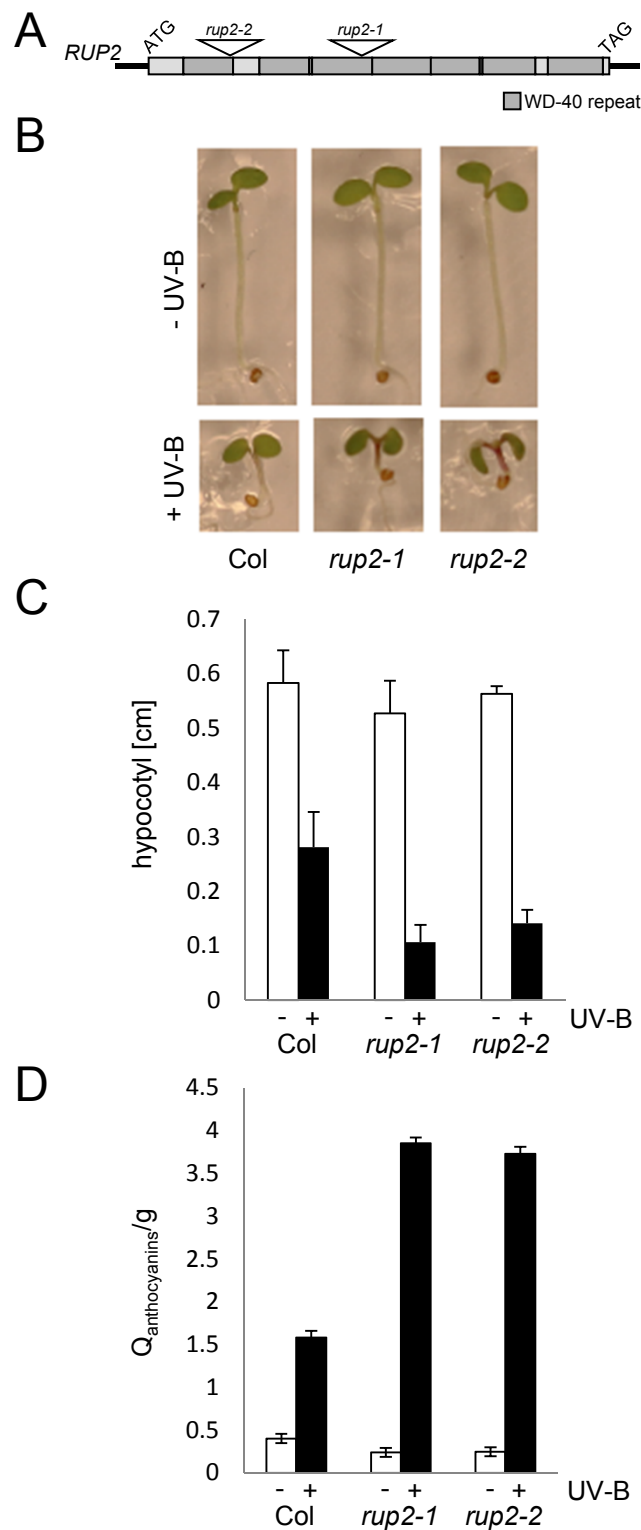
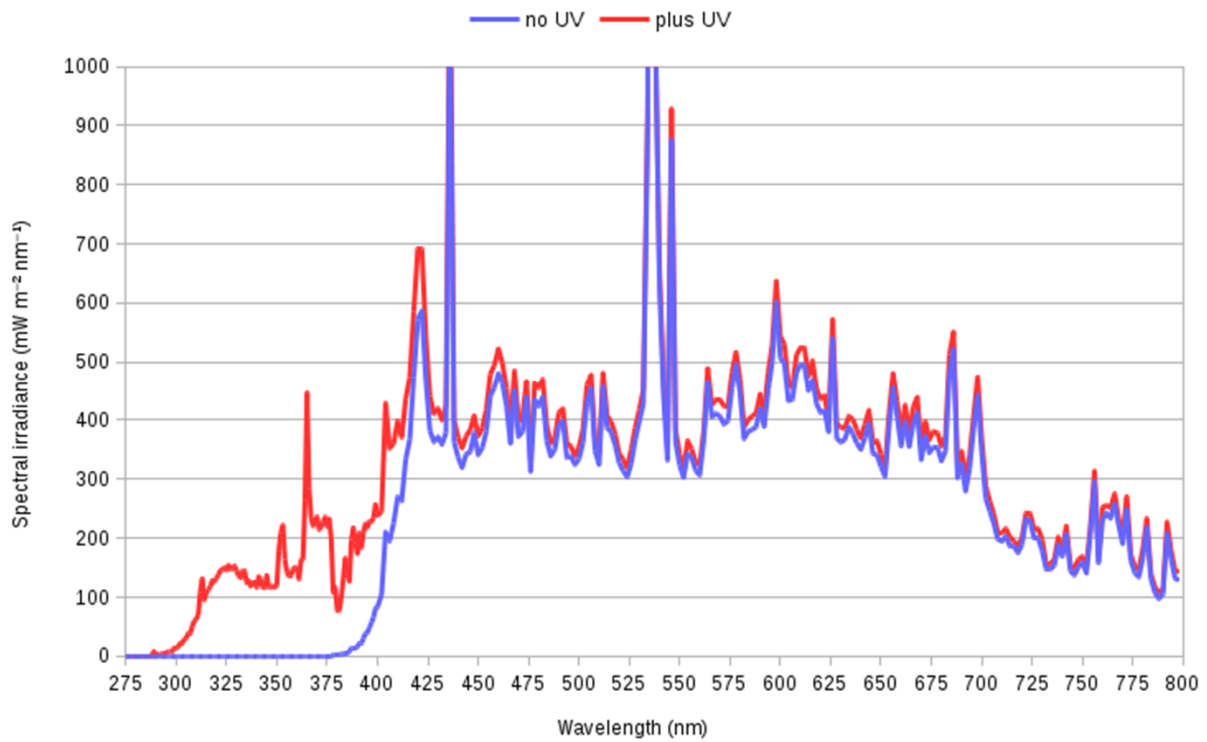


**Figure S6.** The *rup2-2* mutant allele confers UV-B hypersensitivity, similar to *rup2-1*. (A) Structure of *RUP2*, and the approximate locations of T-DNA insertions in *rup2-1* and *rup2-2*. (B) Representative images showing the UV-B inhibition of hypocotyl length and elevated anthocyanin content (dark red pigmentation) in 4-d-old WT (Col), *rup2-1*, and *rup2-2* seedlings when compared to seedlings grown in weak-white light devoid of UV-B. (C) Hypocotyl length measurements of 4-d-old seedlings grown with (+) or without (-) UV-B. Error bars indicate SEM ( $n = 30$ ). (D) Anthocyanin level of 4-d-old *Arabidopsis* seedlings grown with (+) or without (-) UV-B. Data shown are the mean values of three independent biological replicates. Error bars represent SD ( $n = 3$ ).

A



B

	-UV	+UV
PAR ( $\mu\text{mol m}^{-2} \text{s}^{-1}$ )	580	600
UV-B <sub>BE</sub> ( $\text{mW m}^{-2}$ )	< 0.1	308
UV-C ( $\text{W m}^{-2}$ )	< 1e-04	< 1e-04
UV-B ( $\text{W m}^{-2}$ )	< 1e-04	0.91
UV-B ( $\mu\text{mol m}^{-2} \text{s}^{-1}$ )	< 1e-03	2.34
UV-A ( $\text{W m}^{-2}$ )	0.59	14.14
UV-A ( $\mu\text{mol m}^{-2} \text{s}^{-1}$ )	1.5	42.6

**Figure S7.** Irradiance conditions in the sun simulator. (A) Spectral irradiances of the study in the sun simulator for control and UV treatment. (B) Determined values from spectroradiometric measurements of the irradiance condition in the sun simulator. UV-B<sub>BE</sub>: biologically effective UV-B radiation, normalized at 300 nm (Caldwell 1971).